

ELECTRON MICROSCOPIC STUDIES OF INDUCED CARTILAGE DEVELOPMENT AND CALCIFICATION

H. CLARKE ANDERSON

From the Department of Pathology, State University of New York, Downstate Medical Center,
Brooklyn, New York 11203

ABSTRACT

Cultured, human, amniotic cells (FL strain) injected into the thigh muscles of cortisone-conditioned mice proliferated to form discrete colonies which, over a period of 5 days, became invested by numerous fibroblasts. Cartilage cells and matrix appeared within the fibroblastic zones during the succeeding 2-4 days. Cartilage matrix calcified within 12 days following FL-cell injection. Cartilage cells closely resembled fibroblasts from which they appeared to be derived, and were readily distinguished from FL cells by their prominent ergastoplasm and Golgi complexes. Cartilage matrix was composed of a distinctive feltwork of randomly arranged, collagen fibrils (~ 600 A axial period and ~ 250 A width) from which small electron-opaque, leaflike matrix particles extended. Matrix calcification occurred with the deposition of radially arranged needle-like structures resembling hydroxyapatite. Dense centers were often identified within these clusters. Examination of heavily calcified areas revealed confluent masses of apatite-like material. In general, the fine structure of induced cartilage formation and calcification resembled that of cartilage development and calcification as previously described in the normal epiphysis.

INTRODUCTION

When cultured, human, amniotic cells of the FL strain (1) are injected into the thigh muscles of cortisone-conditioned mice they proliferate to form discrete colonies which, within 12 days of injection, become invested with bone (2). Bone is formed heterotopically through a process resembling endochondral ossification.

Our light microscopic studies suggested that chondrocytes, whose appearance precedes bone formation, were derived from host fibroblasts which accumulated in large numbers around the injected FL cells prior to cartilage formation (3, 4).

Bone formation induced by FL cells was studied by electron microscopy in an attempt to delineate

more clearly fibroblasts from FL cells (5). It was also thought desirable to determine whether this technique might give information on the existence or nonexistence of possible transitional cell types between the obvious FL- and fibroblast cells.

Details of induced cartilage formation and calcification are reported below and are compared to those of previously described normal endochondral ossification (6-16).

MATERIALS AND METHODS

Tumors were produced in cortisone-conditioned 15-g female ICR/Ha mice by intramuscular injection of $1.5-5.0 \times 10^6$ FL, amniotic, tissue-culture cells (2). Animals were sacrificed at intervals (5, 7, 9, and 12 days) following FL-cell inoculation. From 5 to 9 animals were examined at each day of sacrifice.

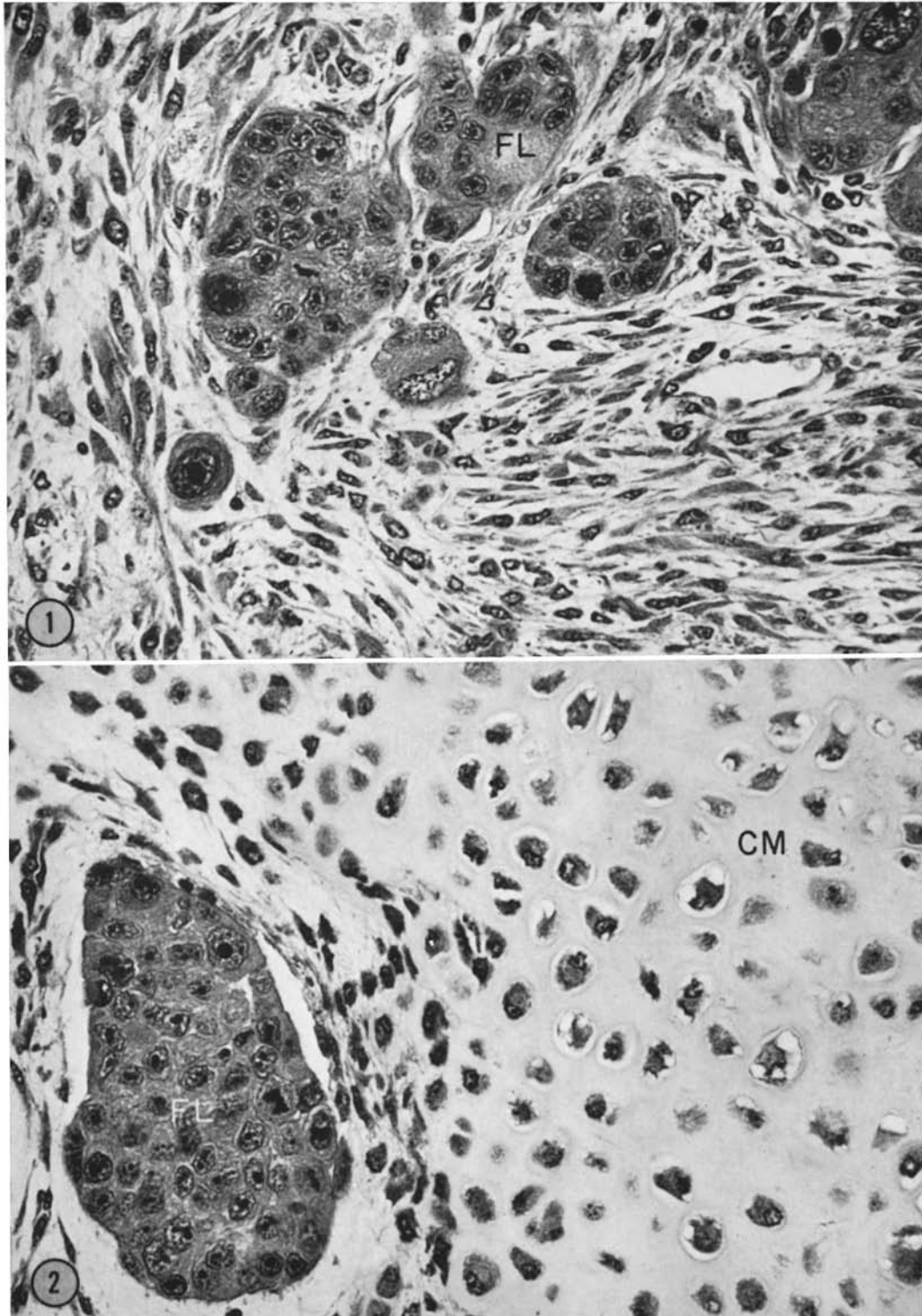


FIGURE 1 Fibroblasts surround colonies of FL cells (FL) 5 days after injection of FL cells. $\times 440$.

FIGURE 2 Cartilage cells and matrix (CM) appear among fibroblasts 7 days after FL cell (FL) injection. Central chondrocytes exhibit hypertrophy. $\times 440$.

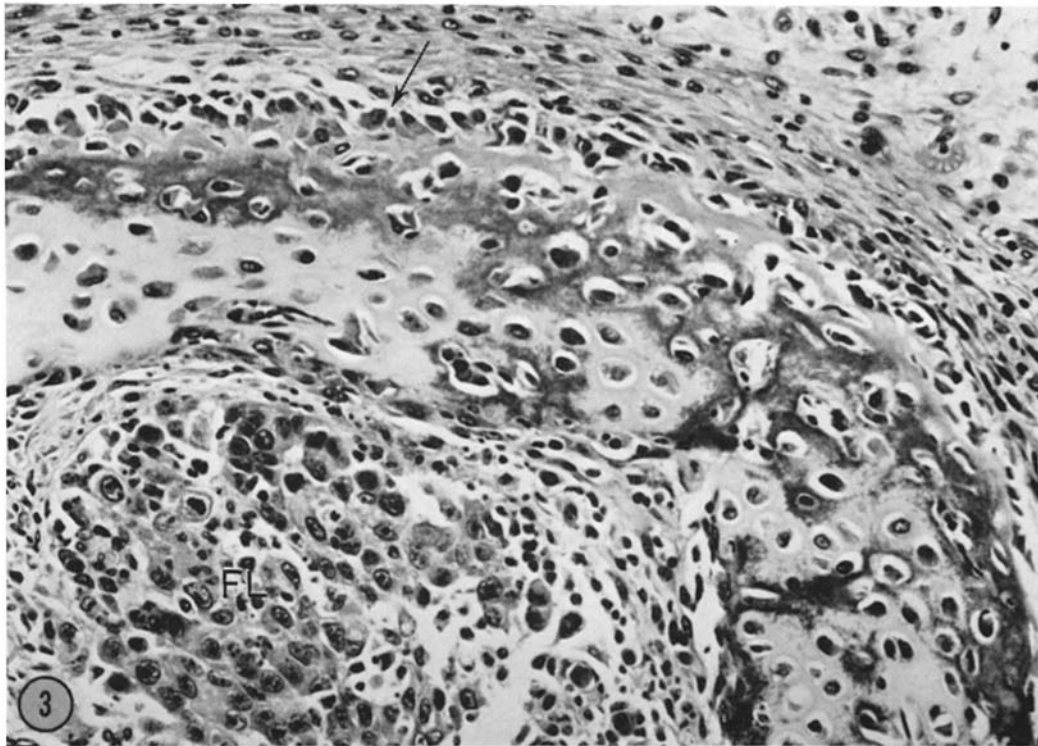


FIGURE 3 Calcium (dark granular material) deposited in cartilage matrix 12 days after FL cell injection, coincident with hypertrophy and degeneration of chondrocytes. Cells resembling osteoblasts are seen at upper margin of the cartilaginous spicule (arrow). $\times 300$.

Tissue Preparation

Tumors were removed, cut into small pieces, and fixed for 2 hr at 4°C in buffered osmium tetroxide (17). In some instance fixation was carried out in 4°C phosphate-buffered glutaraldehyde for 1 hr (18) followed by postfixation for 1 hr in 2% aqueous solution of osmium tetroxide or in buffered osmium tetroxide (17) at 4°C. Cultured FL cells to be examined were detached and sedimented as for injection (2), and then were resuspended as clumps in 4°C osmium-tetroxide fixative (17) for 2 hr. After fixation, tissues were dehydrated in graded alcohols, embedded in Epon, and cut with diamond and glass knives on Porter-Blum and LKB microtomes. Thick-thin sectioning techniques were utilized to locate areas containing FL cells and/or areas of developing cartilage and bone. Thick sections were stained in 1% aqueous solution of toluidine blue containing 1% sodium borate for 15–30 sec and then were washed in running water prior to light microscopic examination.

Several stains were used for thin sections including lead hydroxide (19, 20), lead citrate (21), uranyl acetate (22), and lead citrate (21) preceded by 3% aqueous solution of uranyl acetate for 5 min. Sections

were examined and photographed in an RCA EMU-3F electron microscope. All electron micrographs presented below were obtained from osmium tetroxide fixed tissues (17) stained with lead citrate (21) and aqueous uranyl acetate, unless otherwise specified.

RESULTS

Sequence of Cellular Events As Seen By Light Microscopy

After injection FL cells proliferated to form discrete colonies which over a period of 5 days became surrounded by fibroblasts (Fig. 1). Cartilage formation was observed within fibroblastic zones approximately 7 days after injection of FL cells (Fig. 2). Calcification of cartilage matrix began 2–4 days after the appearance of cartilage (Fig. 3). At this time many chondrocytes underwent hypertrophy and degeneration. Cells resembling osteoblasts were seen frequently at the margins of calcifying spicules of cartilage matrix (Fig. 3).

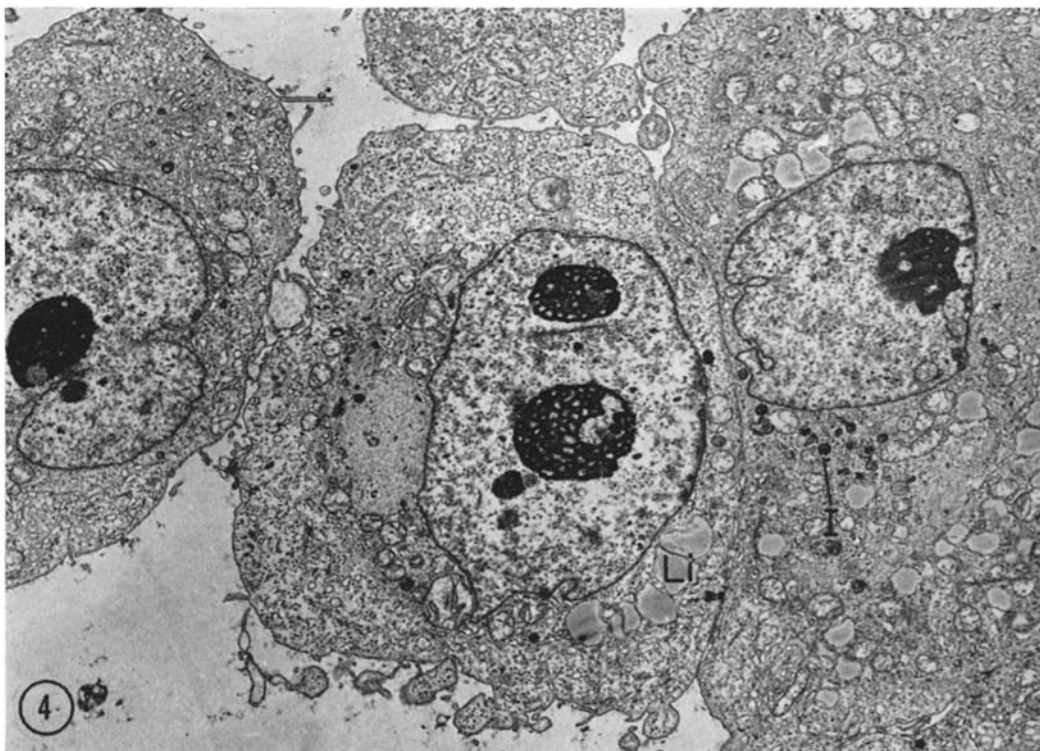


FIGURE 4 FL cells in culture demonstrating large irregular nuclei and nucleoli, reduced ergastoplasm, and scattered, small, dense, membrane-bounded inclusions (*I*). Lipid droplets (*Li*) appear more numerous in cultured than in injected FL cells of Fig. 5. $\times 3400$.

Electron Microscopic Differentiation of FL Cells and Fibroblasts

Differences between FL cells and fibroblasts were studied. FL cells (Figs. 4-7) were larger and rounder than fibroblasts and, *in vivo*, were in contact with one another over most of their exposed surfaces (Fig. 5). FL-cell adherence was maintained by typical desmosomal attachments (maculae adhaerentes) (Fig. 6). FL-cell nuclei were large and frequently showed deep indentations. Their nucleoli tended to be large and irregular. The FL-cell cytoplasm was abundant and contained numerous, free, ribosomal rosettes as well as a few profiles of rough-surfaced endoplasmic reticulum (Fig. 6). The FL-cell Golgi complex was small and inconspicuous. Many FL cells contained intracytoplasmic membrane-bounded inclusions which varied in size from small, electron-opaque structures (Figs. 4, 5) to large aggregates containing partially disrupted

cell organelles (Fig. 7). The plasma membrane was usually smooth except at the unattached surfaces of FL-cell colonies where irregular microvillous projections were seen (Fig. 6).

Fibroblasts were smaller, more elongate, and without much surface contact with other cells (Fig. 8). Frequently they were separated by a collagenous matrix. True desmosomes (maculae adhaerentes) were not identified between adjacent fibroblasts, or between fibroblasts and FL cells. Fibroblast nuclei were smaller and more elongate and contained smaller nucleoli. The fibroblast cytoplasm contained prominent ergastoplasm and an extensive Golgi complex. Large polymorphous inclusions, seen frequently in FL cells, were extremely rare in fibroblasts. The plasma membrane of fibroblasts showed some undulation as well as occasional microvillous projections.

Cytological features common to both FL cells and fibroblasts included multivesicular bodies,

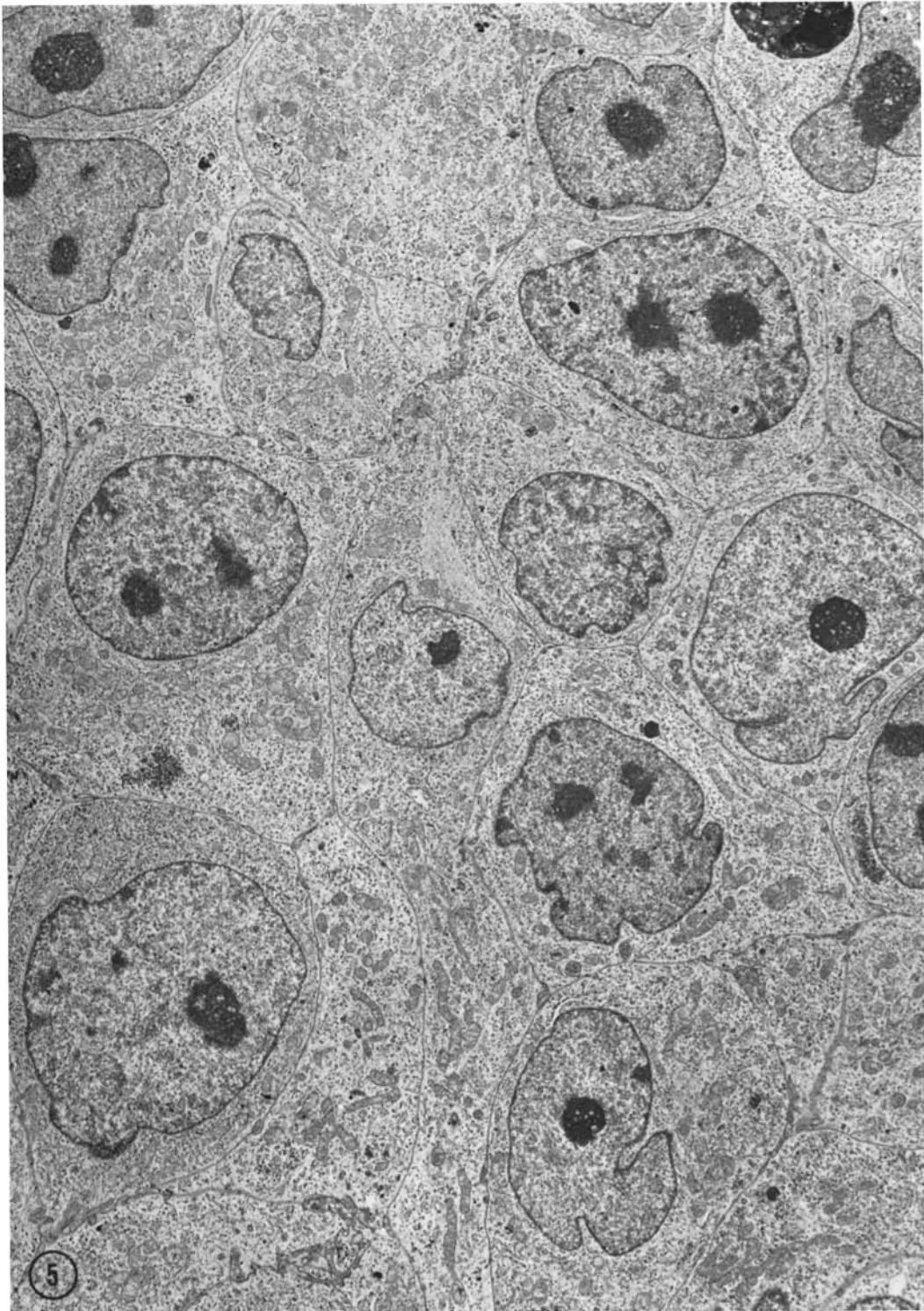


FIGURE 5 Injected FL cells demonstrating typical adherence, polygonal shape, large irregular nuclei and nucleoli, and reduced ergastoplasm and Golgi complexes. A few small membrane-bounded cytoplasmic inclusions are present. $\times 3400$.

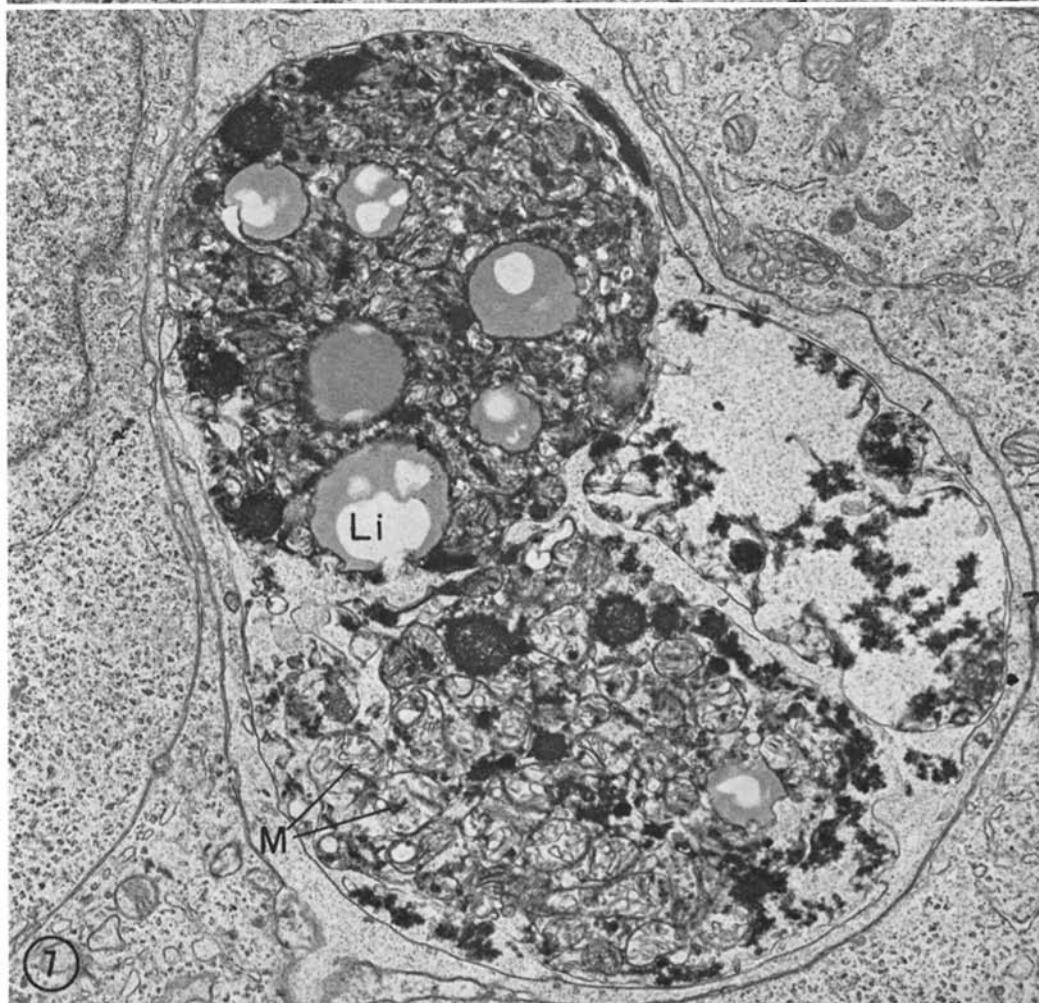
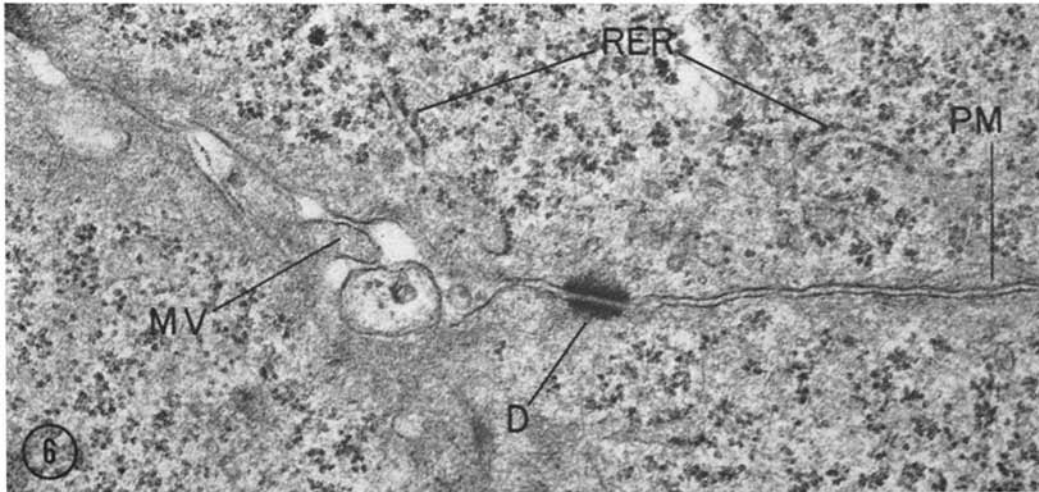


FIGURE 6 FL cell junction with a desmosome (*D*). There is focal folding of the plasma membrane (*PM*) into microvilli (*MV*). The cytoplasm contains many free ribosomal rosettes and sparse ergastoplasm (*RER*). (Glutaraldehyde fixation with postosmication). $\times 38,500$.

FIGURE 7 Polymorphous membrane-bounded inclusion containing intact and degenerated mitochondria (*M*), membranes and lipid (*Li*) within the cytoplasm of an FL cell. $\times 38,500$.

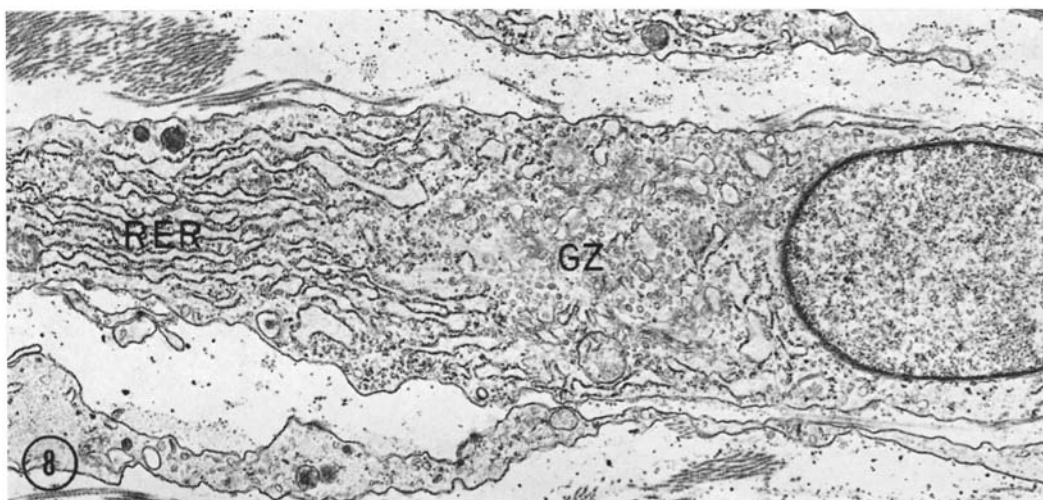


FIGURE 8 Fibroblast showing typical elongate configuration, nonadherence, and prominent ergastoplasm (RER), and Golgi zone (GZ). $\times 10,700$.

small membrane-bounded inclusions, and bundles of cytoplasmic fine filaments ~ 80 Å in diameter.

From the above described features fibroblasts could be distinguished readily from FL cells, and no transitional forms between the two types were recognized.

Other Cell Types

Histiocytes were frequently intermixed with fibroblasts during the early stages of fibroblastic proliferation and could be distinguished by the presence of numerous pinocytic vesicles and membrane-bounded, electron-opaque bodies within the cytoplasm (Fig. 9). Ergastoplasm was less well-developed in histiocytes than in fibroblasts, although Golgi complexes were prominent. Histiocytes were rare in cartilaginous zones.

Polymorphonuclear leukocytes also were present in varying numbers and could be recognized by their lobulated nuclei and characteristic cytoplasmic granules.

Cellular Changes During Chondrogenesis and Calcification

Cartilage cells (Fig. 10) appeared within fibroblastic zones 7 days after FL-cell injection. Although more rounded in configuration, they bore a striking resemblance to fibroblasts. The chondrocyte ergastoplasm was well developed, as

was the Golgi complex which showed prominent dilatation of Golgi vesicles containing small granules and twisted interlacing fibrils ~ 80 Å in diameter (Fig. 11). Some chondrocytes contained glycogen-like material. Intracytoplasmic lipid appeared reduced in chondrocytes as compared to fibroblasts.

Hypertrophy and associated degeneration of chondrocytes occurred at about the same time as matrix calcification (9–12 days after FL-cell injection). During this process some chondrocytes underwent shrinkage and condensation (Fig. 12), associated with a striking accumulation of intracytoplasmic glycogen (Figs. 12 and 13).

Swelling of chondrocytes was also observed during the period of hypertrophy and degeneration (Fig. 14). This process was usually associated with decreased cytoplasmic density and marked dilatation of rough-surfaced endoplasmic reticulum. Occasionally ergastoplasmic profiles were seen which occupied as much or more space than that occupied by a normal chondrocyte (Fig. 15). In this instance contents of ergastoplasmic profiles appeared less concentrated, and ~ 80 Å-wide filaments and small granules could be resolved (Fig. 16).

Degenerating chondrocytes underwent lysis with plasma membrane rupture (Fig. 17) and dispersal of cell fragments into the interstices of the cartilaginous matrix (Fig. 18).

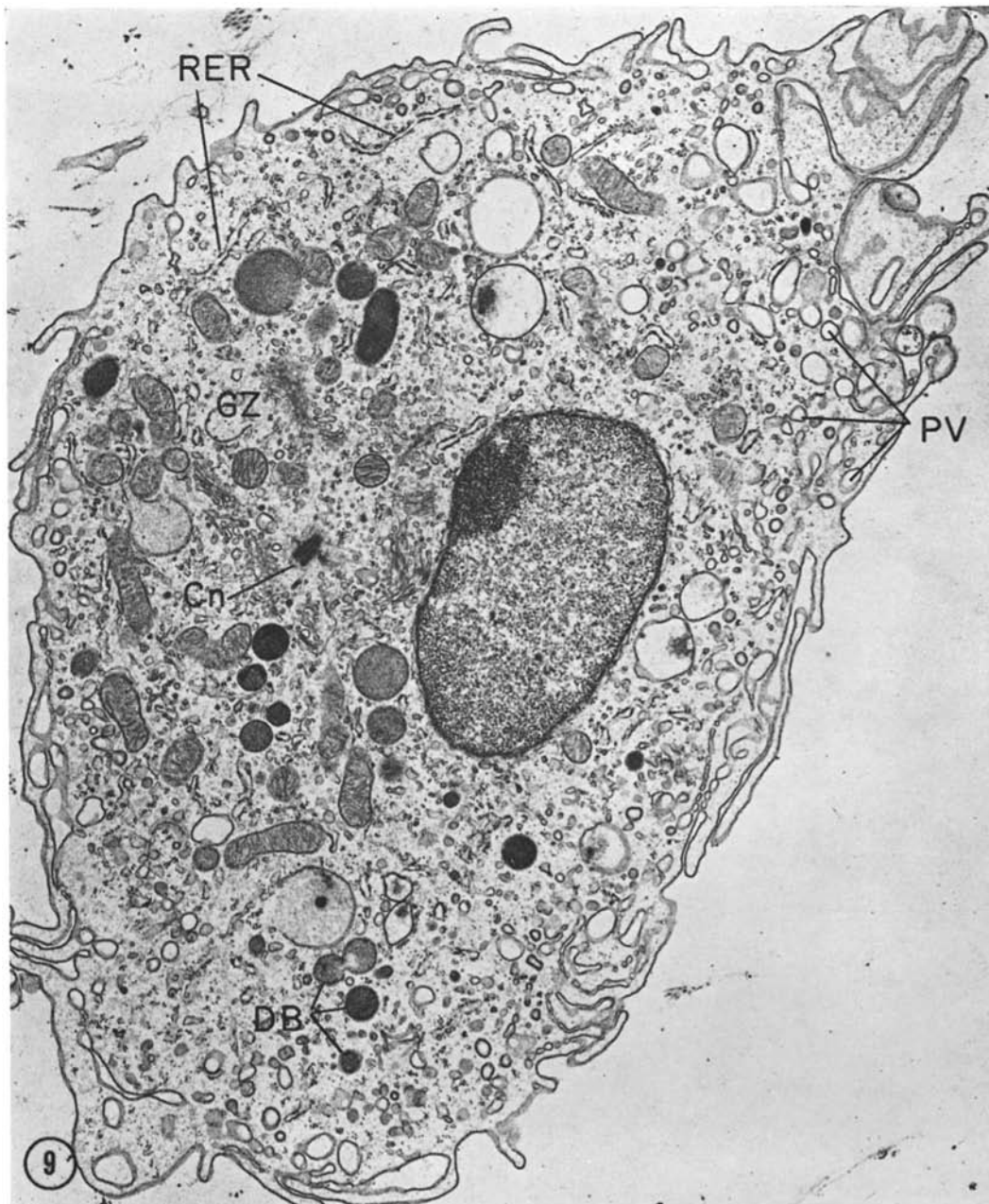


FIGURE 9 Histiocyte containing multiple pinocytic vesicles (*PV*), membrane-bounded dense bodies (*DB*), prominent Golgi apparatus (*GZ*), and reduced rough endoplasmic reticulum (*RER*). A centriole (*Cn*) is present in the Golgi zone. $\times 11,400$.

*Intercellular Matrix: Cartilage
Versus Noncartilage*

Cartilage matrix was composed of a distinctive feltwork of randomly arranged collagen fibrils

(Fig. 19) showing a ~ 600 A major axial period and ~ 250 A diameter. At least eight intraperiod bands could be identified in larger collagen fibrils.

Leaflike electron-opaque particles were present

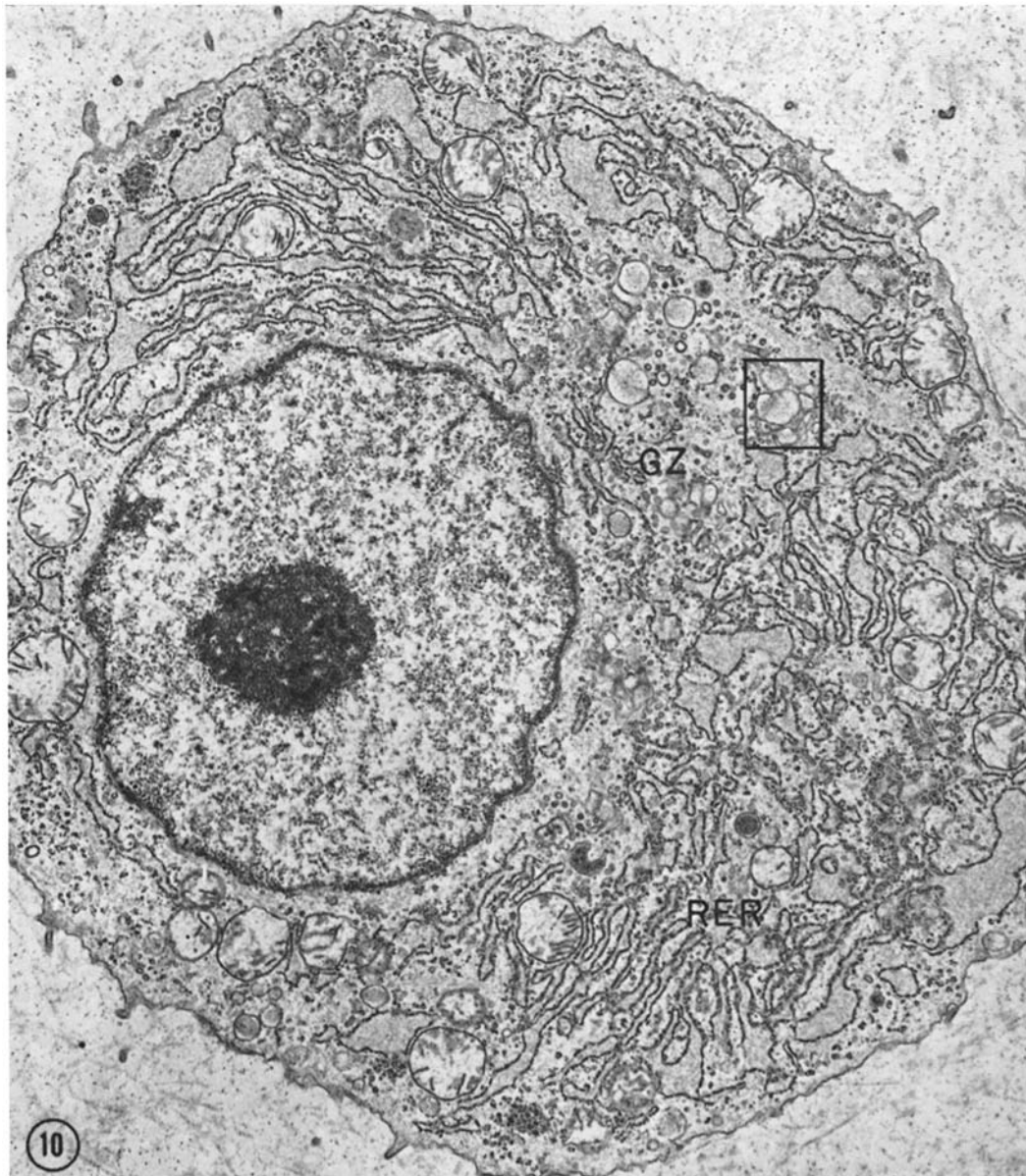


FIGURE 10 Chondrocyte surrounded by cartilage matrix containing prominent rough endoplasmic reticulum (*RER*) and dilated vesicles in the Golgi zone (*GZ*). Golgi vesicles, similar to those enclosed by the rectangle, are represented in detail in Fig. 11. $\times 7,900$.

in cartilage matrix, and often extended from attachment points on collagen fibrils (Fig. 19). These structures measured ~ 350 A in length, and varied in width from ~ 40 – 200 A. They were somewhat fusiform in shape, projected into the interfibrillar space at irregular angles, and fre-

quently appeared to taper into fibrillar extensions. They were identified after osmium tetroxide- or glutaraldehyde-fixation (with or without post-osmication) and after staining with lead hydroxide, lead citrate, and/or uranyl acetate.

In noncartilaginous areas, and in early fibro-

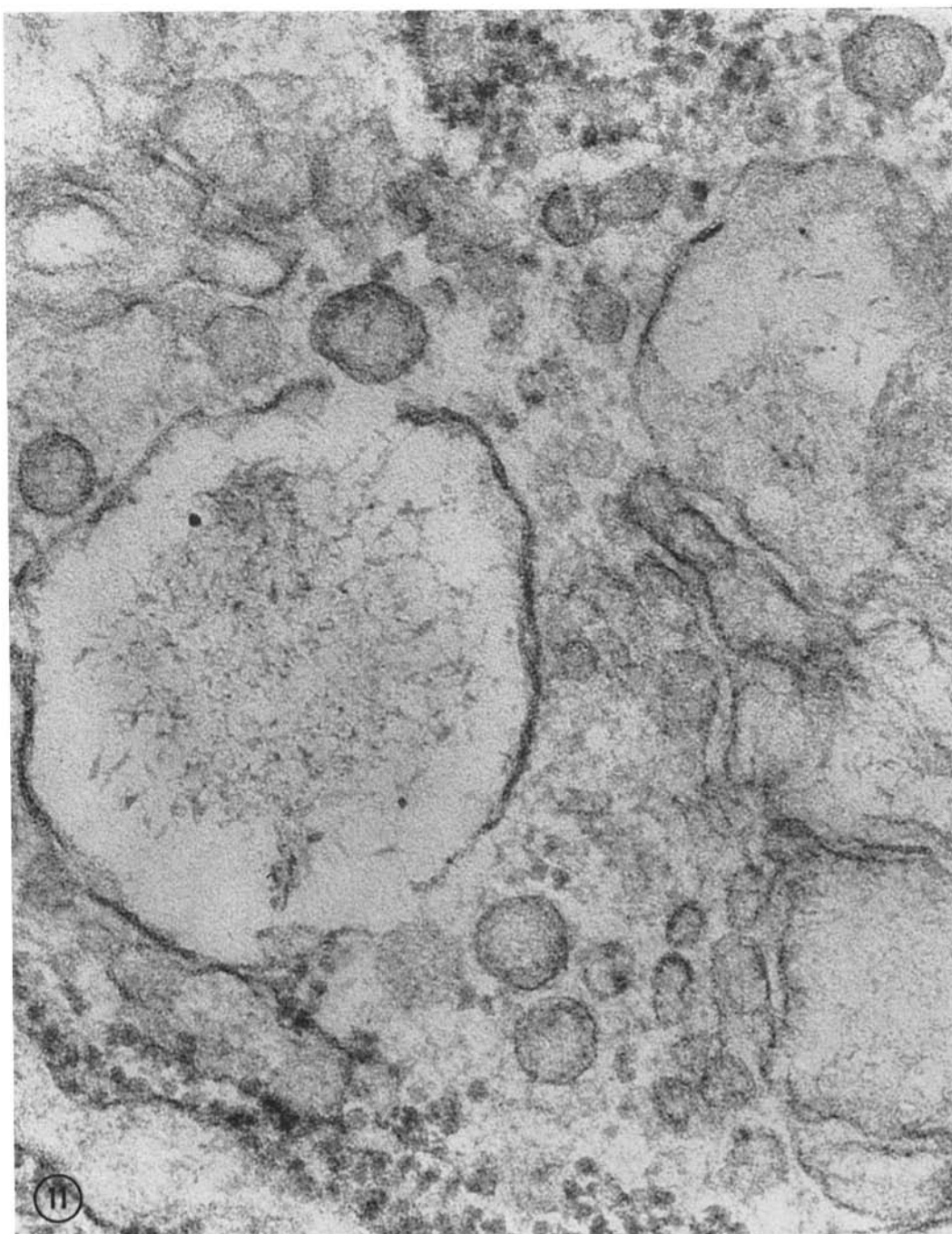


FIGURE 11 Fibrillar and granular material within Golgi vesicles of a chondrocyte (comparable to rectangle in Fig. 10). $\times 144,000$.

blastic response before cartilage development, collagen fibrils often were present in parallel bundles (Fig. 20). These fibrils were divisible into at least two types (Figs. 20 and 21): (a) large

fibrils with ~ 600 Å major axial period and ~ 400 Å diameter, and (b) small fibrils with a ~ 150 Å axial period and a ~ 150 Å diameter. Large and small fibrils were seen often in association, al-

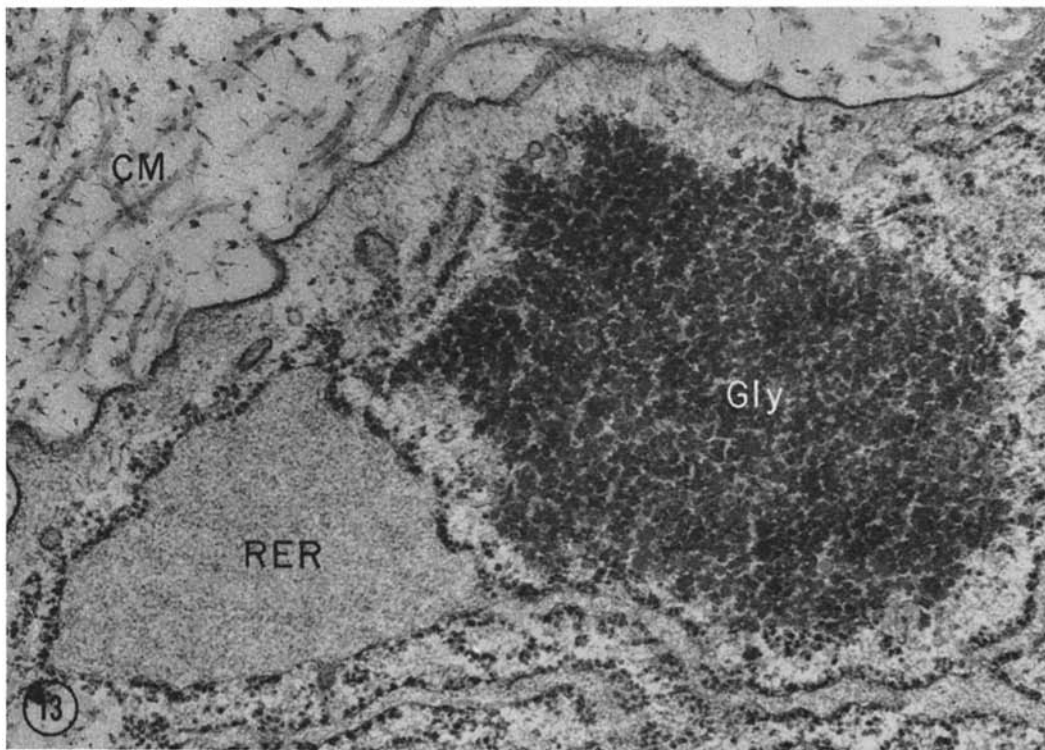
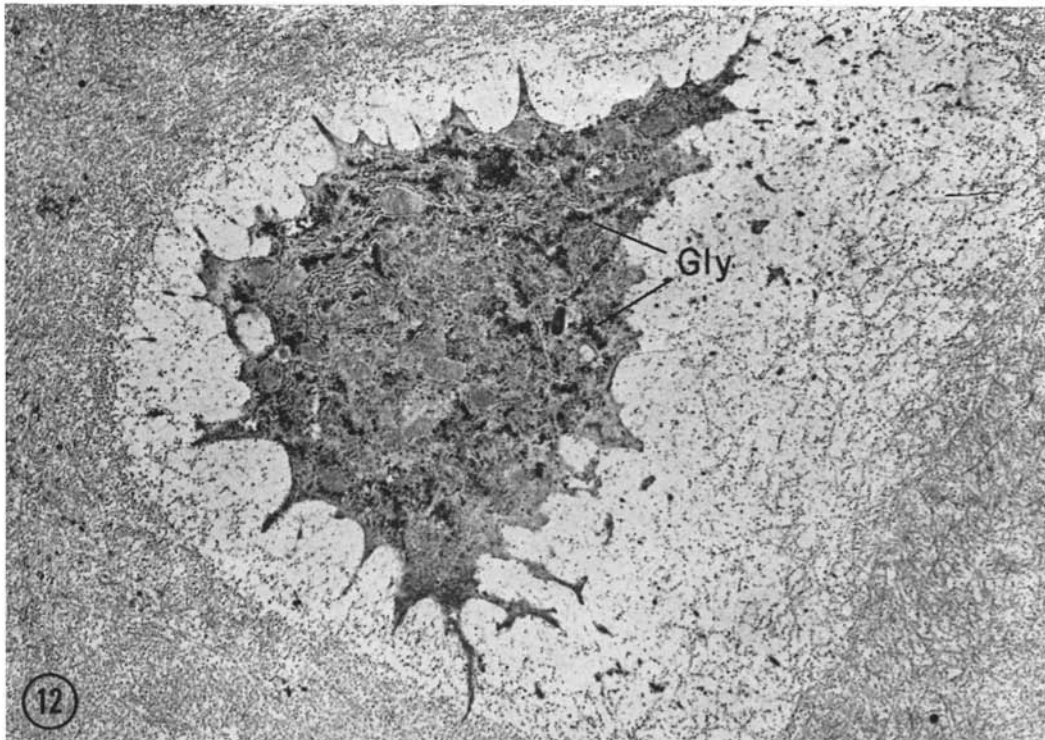


FIGURE 12 Shrinking "spider" chondrocyte, located in an area of chondrocyte hypertrophy and degeneration, showing accumulated intracytoplasmic glycogen-like material (*Gly*) and a surrounding halo of rarified matrix. $\times 5,500$.

FIGURE 13 Cytoplasm of hypertrophic chondrocyte containing glycogen-like material (*Gly*) and dilated ergastoplasm (*RER*). *CM*, cartilage matrix. $\times 39,700$.

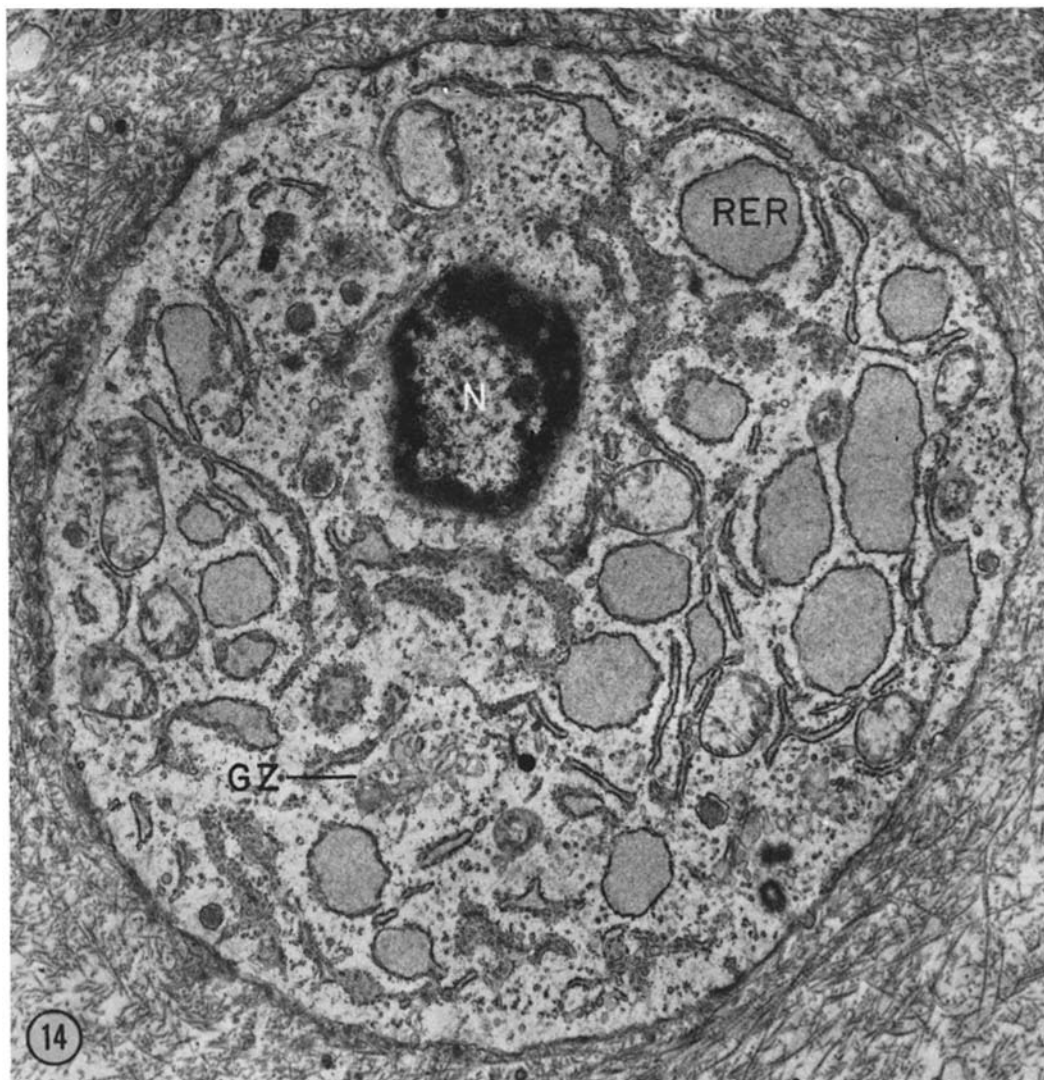


FIGURE 14 Expanded chondrocyte in an area of cartilage cell hypertrophy and degeneration demonstrating markedly dilated rough endoplasmic reticulum (*RER*). *N*, nucleus; *GZ*, Golgi zone. $\times 11,400$.

though each type tended to be concentrated into groups of homogeneous fibril diameter.

Small fibrils measuring from ~ 50 to 100 Å in diameter, without a discernible axial period, were seen in cartilage and in noncartilaginous matrices but were more frequently observed in 5-day noncartilaginous areas.

Leaflike dense particles seen in cartilage matrix, were usually absent from noncartilaginous collagen fibrils arranged in condensed parallel

bundles with smaller interfibrillar distances (Fig. 20).

Early stages of calcification were observed as radial clusters of electron-opaque needle-like structures resembling hydroxyapatite crystals previously described and depicted in bone collagen (Fig. 22). These clusters appeared to be localized over sectioned profiles of collagen bundles. Rounded, dense centers were often identified within the clusters (Fig. 22). Areas of

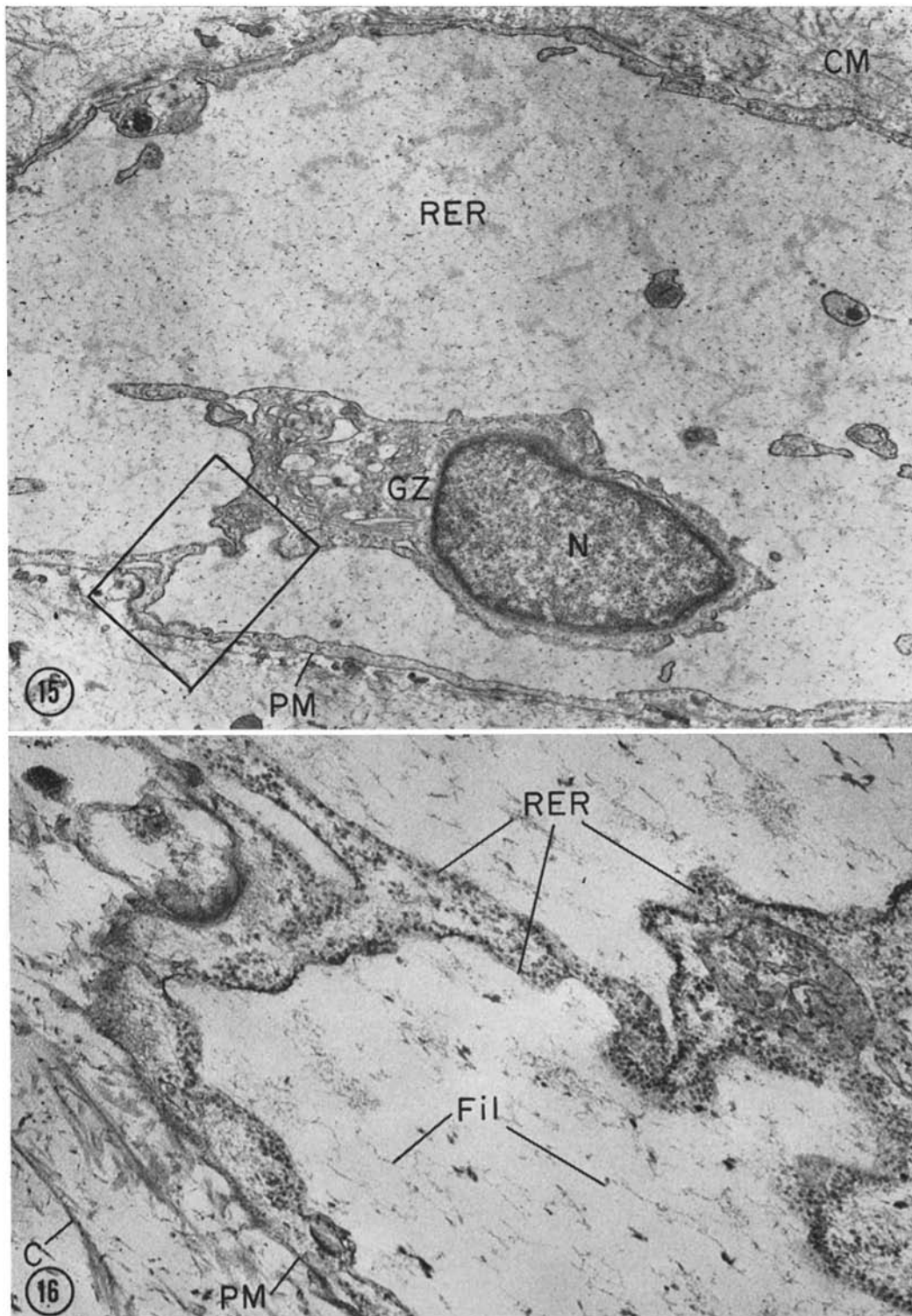


FIGURE 15 Hypertrophic chondrocyte with massively dilated rough endoplasmic reticulum (*RER*). Rectangular area, lower left, shown in detail in Fig. 16. *PM*, plasma membrane; *CM*, cartilage matrix; *GZ*, Golgi zone; *N*, nucleus. $\times 7,900$.

FIGURE 16 Dilated cisternae of rough endoplasmic reticulum (*RER*) (in hypertrophic chondrocyte of Fig. 15) lined by ribosomes and containing filamentous (*Fil*) and granular material. The plasma membrane (*PM*) is surrounded by extracellular collagen fibrils (*C*). $\times 39,700$.

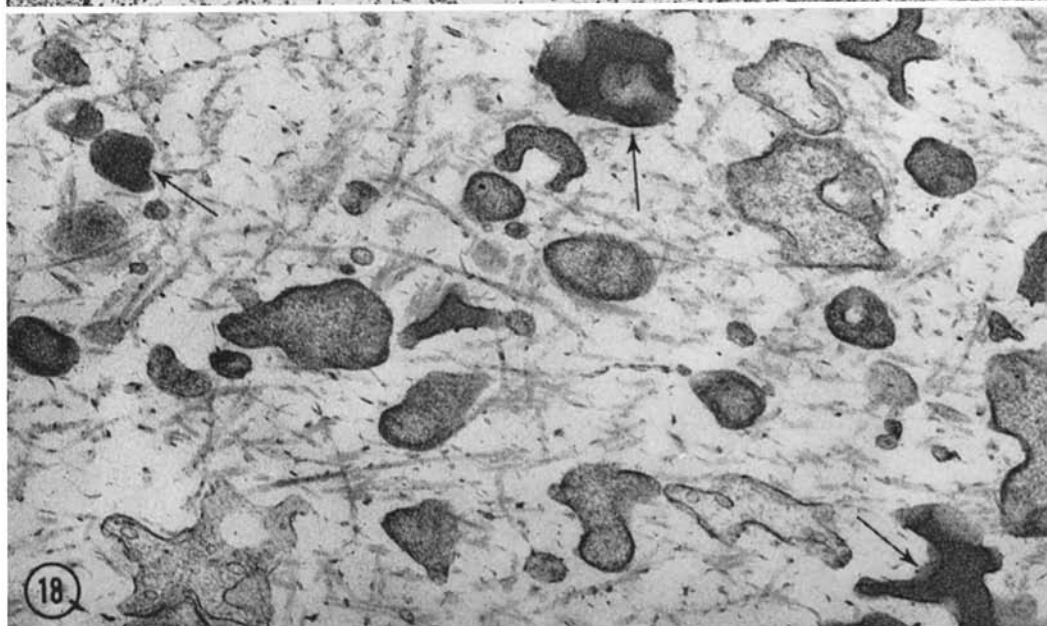
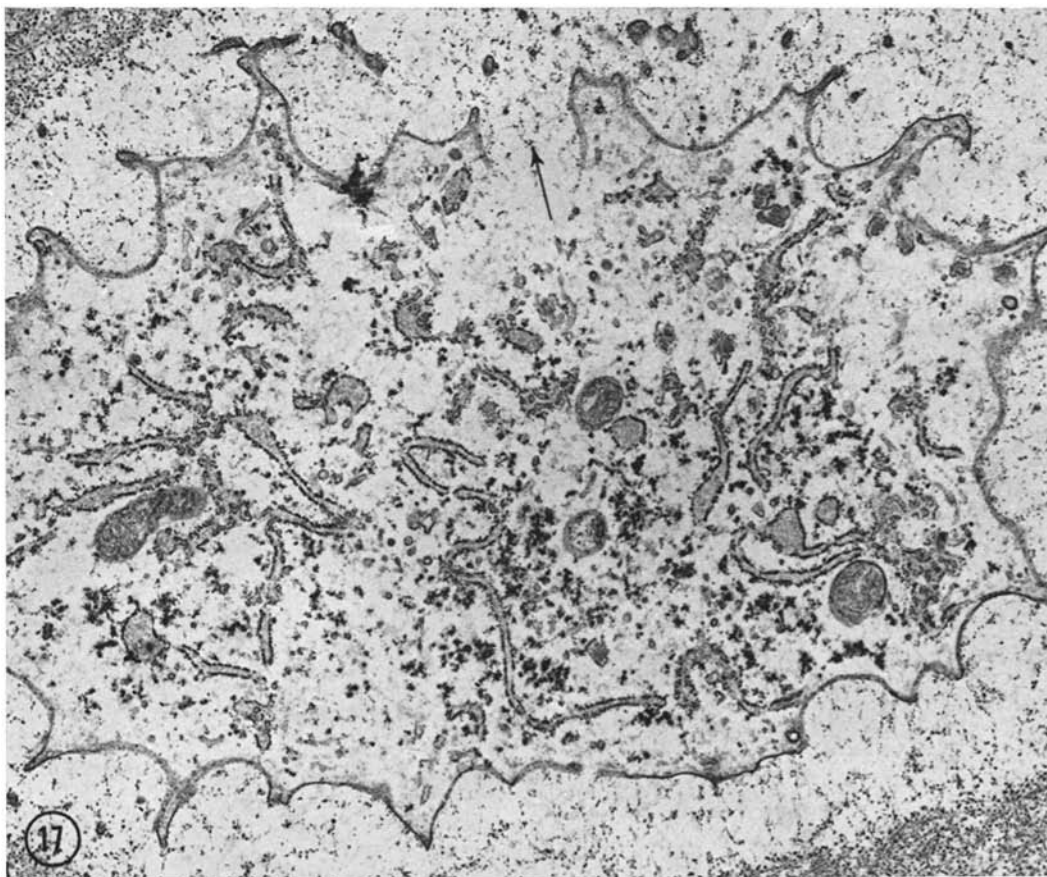


FIGURE 17 Plasma-membrane rupture (arrow) in a degenerating chondrocyte. $\times 11,400$.

FIGURE 18 Membrane-bounded cytoplasmic fragments in matrix of hypertrophic cartilage. Some fragments appear to contain lipid (arrows). $\times 36,000$.

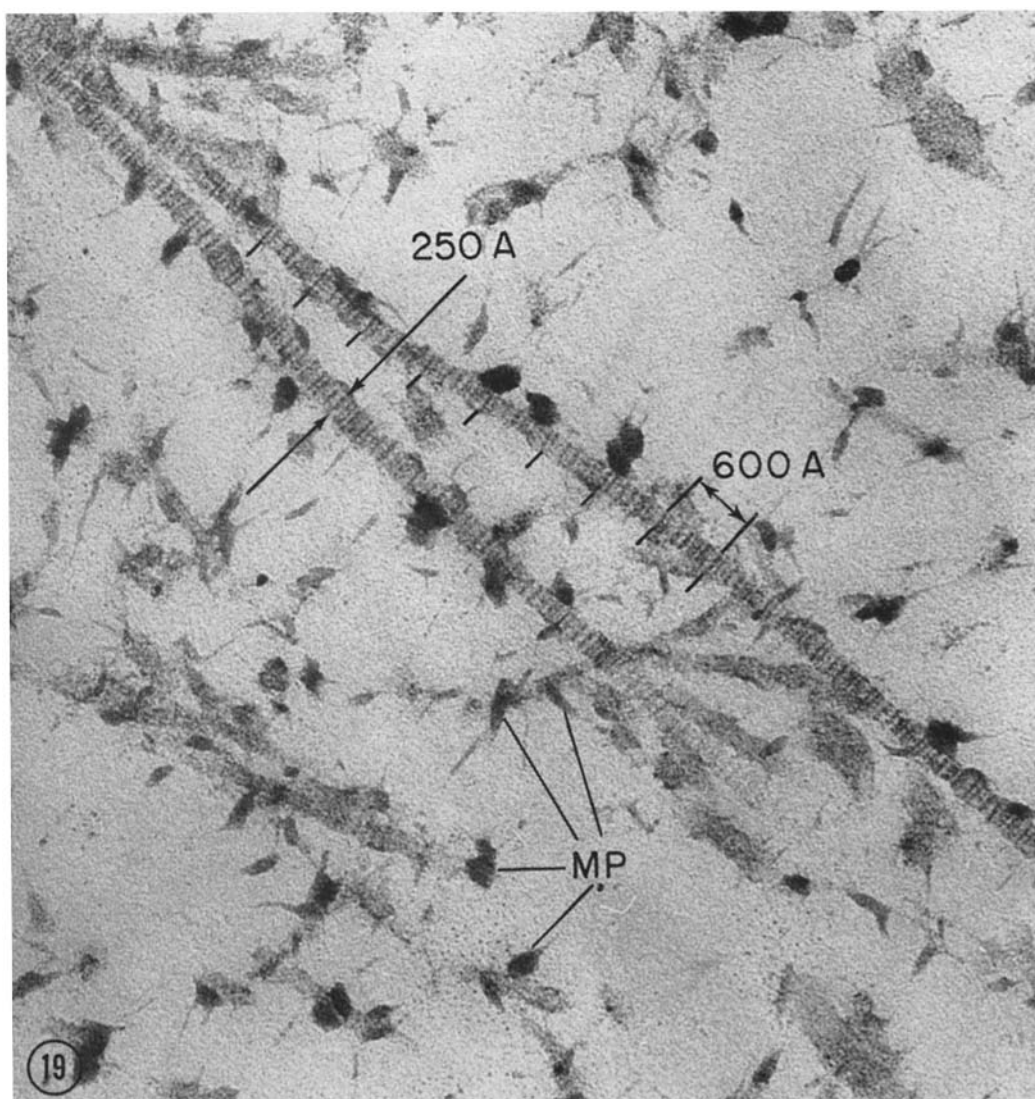


FIGURE 19 Cartilage matrix with randomly disposed collagen fibrils (~ 600 A estimated axial period and ~ 250 A width) separated by large interfibrillar distances. Note dense, leaflike matrix particles (*MP*) frequently attached to collagen fibrils. Stellate fibrillar projections extend from many matrix particles. $\times 144,000$.

heavy calcification contained confluent masses of apatite-like material (Fig. 23).

DISCUSSION

Role of FL Cells and Fibroblasts in Bone Formation

FL cells were readily distinguished from surrounding fibroblasts by electron microscopy (5, 23,

24) as they were with other techniques of histochemistry and radioautography (3, 4). The fact that transitional forms between the two cell types were not recognized is in agreement with earlier studies employing tritium-labeled FL cells (3, 4) which suggested that the FL cells did not transform into fibroblasts. Since FL cells apparently do not transform into bone-forming fibroblasts and do not themselves elaborate a cartilaginous matrix

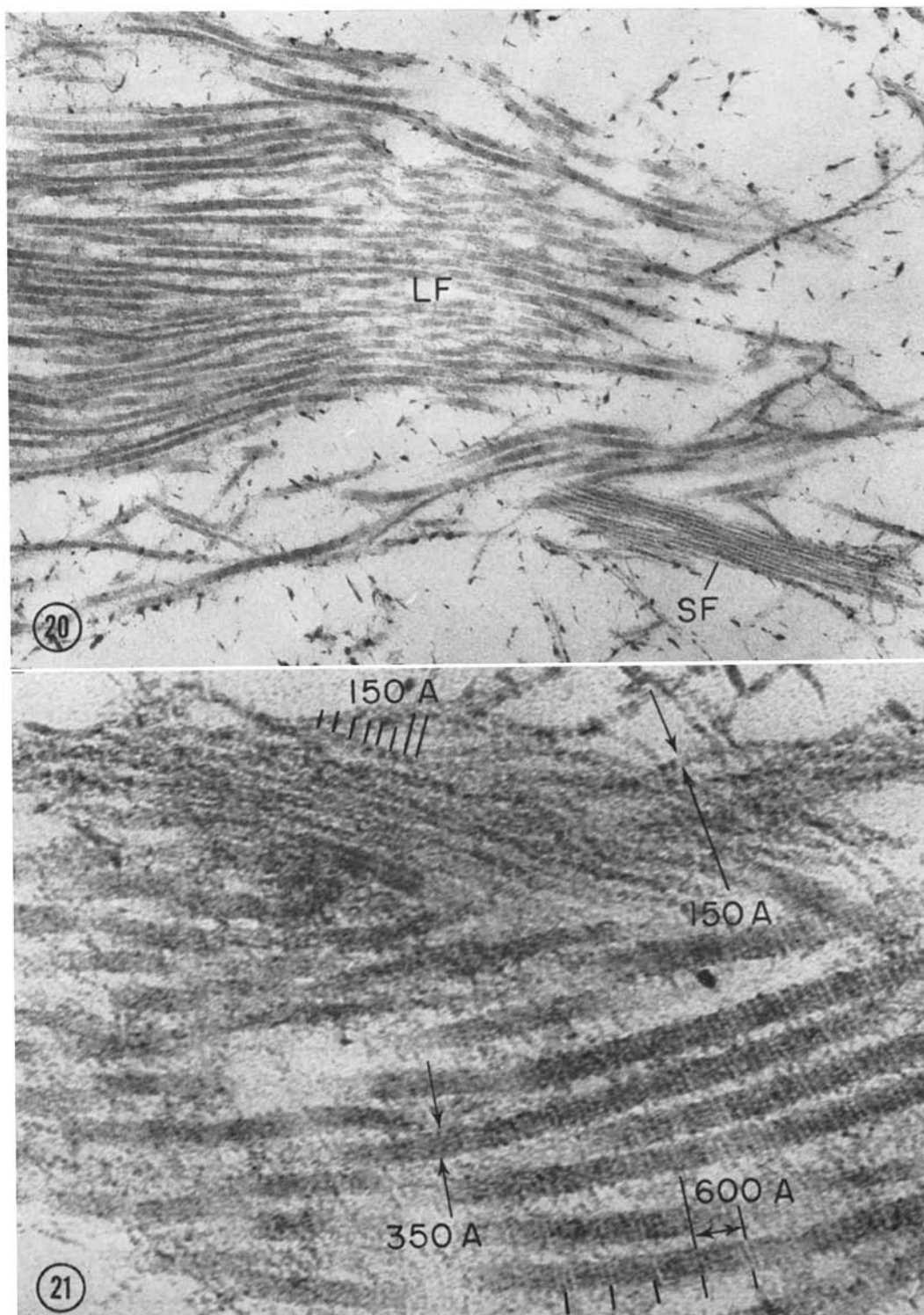


FIGURE 20 Noncartilaginous collagen with large fibrils (*LF*) and small fibrils (*SF*) arranged in condensed parallel bundles. Note absence of matrix particles from condensed bundles. $\times 39,700$.

FIGURE 21 Detail of noncartilaginous collagen with large fibrils (~ 600 A period, ~ 350 A width) and small fibrils (~ 150 A period, ~ 150 A width). $\times 144,000$.

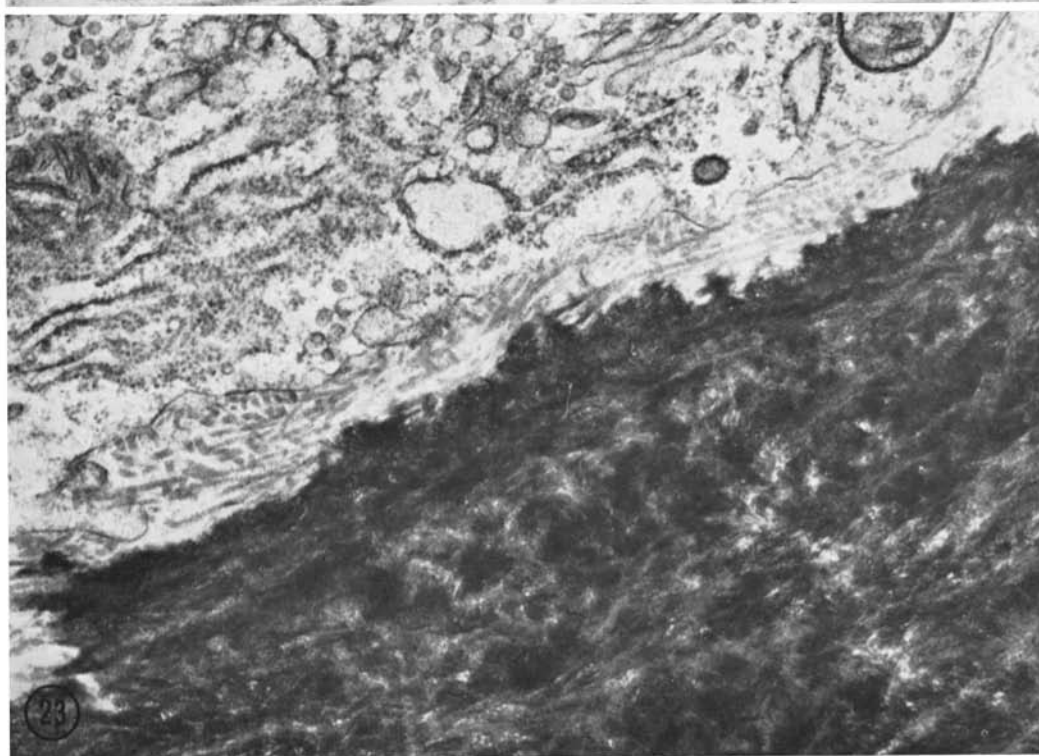
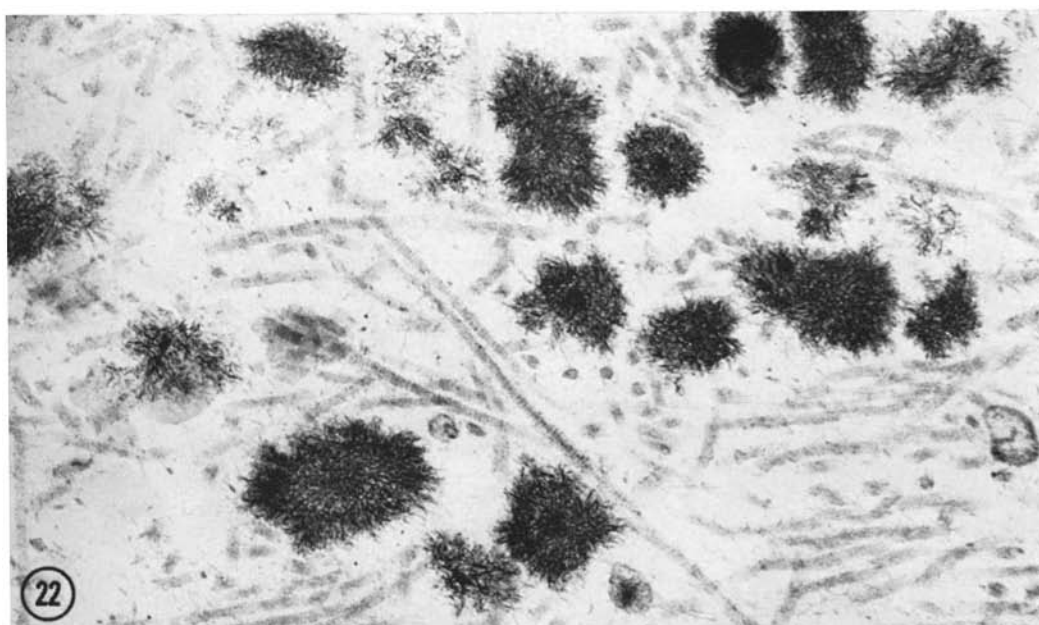


FIGURE 22 Early calcification of cartilage matrix with deposition of radial clusters of needle-like structures resembling hydroxyapatite. Clusters frequently contain central densities. $\times 51,000$.

FIGURE 23 Area of heavy calcification (lower right) showing aggregation of apatite-like material to form a confluent mass. $\times 32,000$.

(3, 4), it would appear that they act by inducing host fibroblasts to undergo cartilage- and bone formation.

That cartilage development occurred focally within the fibroblastic zones surrounding FL cells suggests that cartilage cells were derived from host fibroblasts. Electron microscopy has demonstrated striking similarities between fibroblasts and chondrocytes (24) which are almost identical at the ultrastructural level; this adds evidence to the postulated origin of the latter from the former.

The Chondrocyte Golgi Complex

Although chondrocytes greatly resembled fibroblasts, from which they appeared to be derived, they could be distinguished by their rounded shape and cystic, dilated Golgi complexes containing granular and finely fibrillar material. Hypertrophy of the Golgi apparatus has been described in chondrocytes from a variety of sources (6, 12, 25-30). Granular material (12, 28) and fine nonperiodic filaments (25, 28) also have been identified within chondrocyte Golgi vesicles and correspond to the material seen in the induced chondrocytes. Since the Golgi apparatus has been shown to concentrate and store secretory products (31, 32), it is likely that Golgi complexes in chondrocytes contain material, such as sulfated mucopolysaccharides (33), precollagen (28), or both, destined for secretion into the surrounding cartilage matrix.

Hypertrophic and Degenerating Chondrocytes

Both shrinkage and swelling of chondrocytes were observed during the phase of chondrocyte hypertrophy and degeneration. This process occurred in association with matrix calcification, as is seen at the normal epiphysis (8).

With shrinkage there was a striking, apparent increase in intracytoplasmic glycogen. This phenomenon of glycogen accumulation in hypertrophic and/or senescent chondrocytes is well known (6, 9, 12, 34, 35), and a role in matrix calcification has been suggested (9, 34).

Swelling of hypertrophic chondrocytes was observed as has been described previously (6, 15, 16). With swelling, cystic dilation of the rough-surfaced endoplasmic reticulum was seen often. In some instances the ergastoplasmic contents appeared less concentrated and thus yielded a clearer picture of the fibrillar elements known to be present in the ergastoplasm of chondrocytes (28,

29). These apparently nonperiodic, ~80 A-wide fibrils were similar in many ways to fibrils seen within the Golgi apparatus. They could represent some form of precollagen, as is generally accepted to be present in the rough-surfaced endoplasmic reticulum of collagen-secreting cells (28, 36-40).

Cartilage Cell Fragmentation

Chondrocyte rupture occurred in induced cartilage in association with the appearance of membrane-bounded cell fragments and lipid bodies in adjacent cartilage matrix. Such degeneration and fragmentation of senescent chondrocytes is known to occur at the epiphysis (8, 11, 12, 15, 16). It has also been suggested that discharge of intracellular materials into the matrix may play a role in the coincident process of calcification (7, 11).

Extracellular lipid deposits within the matrix, such as those described above in association with induced cartilage cells, have been recognized in the matrix of articular cartilage (41) and in association with senescent, tracheal chondrocytes (42).

Cartilaginous and Noncartilaginous Matrices

Cartilage matrix was readily recognized by its random distribution of collagen fibrils and by its wide interfibrillar spaces which probably contained large quantities of a protein-mucopolysaccharide complex (43, 44). Collagen fibrils in cartilage generally showed a smaller diameter than the large fibrils seen in noncartilaginous areas where an apparent bimodality of fibril width was observed (large fibrils = ~400 A, and small fibrils = ~150 A in diameter).

The smaller fibrils were usually seen outside of cartilage matrix, frequently in association with parallel bundles of mature collagen fibrils. Similar, small banded or beaded fibrils have been observed in a variety of collagenous matrices (37, 38, 45-53). The smallest of these reported fibrils, similar to fibrils seen most frequently in precartilaginous 5-day FL tumors, measured from 50 to 100 A and did not demonstrate a recognizable axial period (38, 45, 49, 52, 54-57). Such small fibrils may represent an early phase in the aggregation of tropocollagen macromolecules (38, 46-48, 50, 54, 56) which, with continued aggregation, will grow to form more mature collagen fibrils.

The dense leaflike matrix particles described above in induced cartilage also have been iden-

tified in developing epiphyseal cartilage of several species (12, 13, 16, 58) and in regenerating limb-bud cartilage of *Amblystoma* (28). Recent evidence indicates the presence of acid mucopolysaccharide and protein within these structures (58). Close association of matrix particles with collagen fibrils has been noted, as well as the presence of fibrillar stellate projections extending from the particles (28, 58). The latter may represent fibrils of immature collagen (28, 58).

Calcification

Deposition of radial clusters of apatite-like material within cartilage matrix induced by FL cells resembles the normal pattern of cartilage cal-

cification as seen at the epiphysis (6, 13-16). In tangential sections apatite-like structures measured $\sim 50 \times 500$ Å and presented a needle-like appearance. It was not possible to determine whether their true three dimensional contour was needle-like (59) or platelike as has been also suggested (60-62).

This work was supported by United States Public Health Service grants CA-10052 and CA-06081.

The author wishes to acknowledge the many helpful suggestions of Dr. Lawrence Herman, and the expert technical assistance of Miss Priscilla Coulter and Mr. Alan Lieberman.

Received for publication 1 March 1967; revision accepted 8 June 1967.

BIBLIOGRAPHY

1. FOGH, J., and R. O. LUND. 1957. Continuous cultivation of epithelial strain (FL) from human amniotic membrane. *Proc. Soc. Exptl. Biol. Med.* **94**:532.
2. ANDERSON, H. C., P. C. MERKER, and J. FOGH. 1964. Formation of tumors containing bone after intramuscular injection of transformed human amnion cells (FL) into cortisone-treated mice. *Am. J. Pathol.* **44**:507.
3. ANDERSON, H. C., and P. R. COULTER. 1965. Induction of cartilage and bone formation in mice by transplanted FL human tissue culture cells. *Federation Proc.* **24**:437.
4. ANDERSON, H. C., and P. R. COULTER. 1967. Bone formation induced in mouse thigh by cultured human cells. *J. Cell Biol.* **33**:165.
5. ANDERSON, H. C. 1966. Electron microscopy of FL cell-induced heterotopic ossification: delineation of FL cells from bone-forming fibroblasts. *Am. J. Pathol.* **48**:16A.
6. ANDERSON, D. R. 1964. The ultrastructure of elastic and hyaline cartilage of the rat. *Am. J. Anat.* **114**:403.
7. CAMERON, D. A. 1963. The fine structure of bone and calcified cartilage. A critical review of the contribution of electron microscopy to understanding of osteogenesis. *Clin. Orthopaed.* **26**:199.
8. FELL, H. B. 1925. The histogenesis of cartilage and bone in the long bones of the embryonic fowl. *J. Morphol.* **40**:417.
9. FOLLIS, R. H., JR., and M. BERTHRONG. 1949. Histochemical studies on cartilage and bone. I. The normal pattern. *Bull. Johns Hopkins Hosp.* **85**:281.
10. FOLLIS, R. H., JR. 1958. Observations on the structure and metabolism of epiphyseal cartilage. *Bull. N.Y. Acad. Med.* **34**:689.
11. FOLLIS, R. H., JR. 1960. Calcification of cartilage. In *Calcification in Biological Systems*. R. F. Sognnaes, editor. American Association for the Advancement of Science, Washington, D. C. 245.
12. GODMAN, G. C., and K. R. PORTER. 1960. Chondrogenesis, studied with the electron microscope. *J. Biophys. Biochem. Cytol.* **8**:719.
13. ROBINSON, R. A., and D. A. CAMERON. 1956. Electron microscopy of cartilage and bone matrix at the distal epiphyseal line of the femur in the newborn infant. *J. Biophys. Biochem. Cytol.* **2**(Suppl.):253.
14. ROBINSON, R. A., and D. A. CAMERON. 1957. The organic matrix of bone and epiphyseal cartilage. *Clin. Orthopaed.* **9**:16.
15. SCOTT, B. L., and D. C. PEASE. 1956. Electron microscopy of the epiphyseal apparatus. *Anat. Record.* **126**:465.
16. TAKUMA, S. 1960. Electron microscopy of the developing cartilaginous epiphysis. *Arch. Oral Biol.* **2**:111.
17. PALADE, G. E. 1952. A study of fixation for electron microscopy. *J. Exptl. Med.* **95**:285.
18. SABATINI, D. D., K. BENSCH, and R. J. BARNETT. 1963. Cytochemistry and electron microscopy. The preservation of cellular ultrastructure and enzymatic activity by aldehyde fixation. *J. Cell Biol.* **17**:19.
19. MILLONIG, G. 1961. A modified procedure for lead staining of thin sections. *J. Biophys. Biochem. Cytol.* **11**:736.
20. WATSON, W. L. 1958. Staining of tissue sections for electron microscopy with heavy metals.

- II. Application of solutions containing lead and barium. *J. Biophys. Biochem. Cytol.* 4:727.
21. REYNOLDS, E. S. 1963. The use of lead citrate at high pH as an electron-opaque stain in electron microscopy. *J. Cell Biol.* 17:208.
22. STEMPAK, J. G., and R. T. WARD. 1964. An improved staining method for electron microscopy. *J. Cell Biol.* 22:697.
23. FOGH, J., and G. A. EDWARDS. 1959. Ultrastructure of primary culture amnion cells and transformed FL cells in continuous culture. *J. Natl. Cancer Inst.* 23:893.
24. ANDERSON, H. C. 1966. Electron microscopy of heterotopic bone formation induced by FL cells. Sixth International Congress for Electron Microscopy. R. Uyeda, editor. Maruzen Co., Ltd., Tokyo. 2:573.
25. DAVIES, D. V., C. H. BARNETT, W. COCHRANE, and A. J. PALFREY. 1962. Electron microscopy of articular cartilage in the young adult rabbit. *Ann. Rheumat. Diseases.* 21:11.
26. HAY, E. D. 1958. The fine structure of blastema cells and differentiating cartilage cells in regenerating limbs of *Amblystoma* larvae. *J. Biophys. Biochem. Cytol.* 4:583.
27. PERSON, P., and D. E. PHILPOT. 1962. Electron microscope study of squid cartilage. In *Electron Microscopy: Fifth International Congress on Electron Microscopy Held in Philadelphia, Pennsylvania, August 29th to September 5th 1962*. Sydney S. Breese, Jr., editor. Academic Press Inc., New York. 2:T-12.
28. REVEL, J. P., and E. D. HAY. 1963. An autoradiographic and electron microscopic study of collagen synthesis in differentiating cartilage. *Z. Zellforsch. Mikroskop. Anat.* 61:110.
29. SILBERBERG, R., M. HASLER, and M. SILBERBERG. 1965. Submicroscopic response of articular cartilage of mice treated with estrogenic hormone. *Am. J. Pathol.* 46:289.
30. ZELANDER, T. 1959. Ultrastructure of articular cartilage. *Z. Zellforsch. Mikroskop. Anat.* 49:720.
31. PALADE, G. E. 1959. Functional changes in the structure of cell components. In *Subcellular Particles*. T. Hyoshi, editor. The Ronald Press Company, New York. 64.
32. SIEKEVITZ, P., and G. E. PALADE. 1960. A cytochemical study on the pancreas of the guinea pig. V. *In vivo* incorporation of leucine-1-¹⁴C into the chymotrypsinogen of various cell fractions. *J. Biophys. Biochem. Cytol.* 7:619.
33. GODMAN, G. C., and N. LANE. 1964. On the site of sulfation in the chondrocyte. *J. Cell Biol.* 21:353.
34. HARRIS, H. A. 1932. Glycogen in cartilage. *Nature.* 130:996.
35. SILBERBERG, R., M. SILBERBERG, and D. FIER. 1964. Life cycle of articular cartilage cells: An electron microscopic study of the hip joint of the mouse. *Am. J. Anat.* 114:17.
36. JACKSON, S. F. 1960. Fibrogenesis and the formation of matrix. In *Bone as a Tissue*. K. Rodahl, J. T. Nicholson, and E. M. Brown, Jr., editors. McGraw-Hill Book Company, New York. 165.
37. KAJIKAWA, K., T. TANI, and R. HIRONO. 1959. Electron microscopic studies of skin fibroblasts of the mouse, with special reference to the fibrillogenesis in connective tissue. *Acta Pathol. Japan.* 9:61.
38. KARRER, H. E. 1960. Electron microscope study of developing chick embryo aorta. *J. Ultrastruct. Res.* 4:420.
39. LOWTHER, D. A., N. M. GREEN, and J. A. CHAPMAN. 1961. Morphological and chemical studies of collagen formation. II. Metabolic activity of collagen associated with subcellular fractions of guinea pig granulomata. *J. Biophys. Biochem. Cytol.* 10:373.
40. ROSS, R., and E. P. BENDITT. 1965. Wound healing and collagen formation. V. Quantitative electron microscope radioautographic observations of proline-H₃ utilization by fibroblasts. *J. Cell Biol.* 27:83.
41. GHADIALLY, F. N., G. MEACHIM, and D. H. COLLINS. 1965. Extracellular lipid in the matrix of human articular cartilage. *Ann. Rheumat. Diseases.* 24:136.
42. MONTAGNA, W. 1949. Glycogen and lipids in human cartilage with some cytochemical observations on the cartilage of the dog, cat and rabbit. *Anat. Record.* 103:77.
43. MEYER, K., P. HOFFMAN, and A. LINKER. 1958. Mucopolysaccharides of costal cartilage. *Science.* 128:896.
44. SHATTON, J., and M. SCHUBERT. 1954. Isolation of a mucoprotein from cartilage. *J. Biol. Chem.* 211:565.
45. CASTOR, C. W., and K. D. MURDEN. 1964. Collagen formation in monolayers of human fibroblasts. The effects of hydrocortisone. *Lab. Invest.* 13:560.
46. CHAPMAN, J. A. 1961. Morphological and chemical studies of collagen formation. I. The fine structure of guinea pig granulomata. *J. Biophys. Biochem. Cytol.* 9:639.
47. CURRAN, R. C., and A. E. CLARK. 1963. Formation and structure of the collagen fibril. *Nature.* 198:789.
48. FRANK, R. 1965. Microscopie électronique de la genèse du collagène dans la papille dentaire. *J. Microscop.* 4:43.
49. GOLDBERG, B., and H. GREEN. 1964. An analysis of collagen secretion by established mouse fibroblast lines. *J. Cell Biol.* 22:227.
50. HAUST, M. D. 1965. Fine fibrils of the extracellu-

- lar space (microfibrils). Their structure and role in connective tissue organization. *Am. J. Pathol.* 47:1113.
51. HAUST, M. D., R. H. MOORE, S. A. BENCOSME, and J. U. BALIS. 1965. Elastogenesis in human aorta, an electron microscopic study. *Exptl. Mol. Pathol.* 4:508.
 52. LOW, F. N. 1962. Microfibrils: fine filamentous components of the tissue space. *Anat. Record.* 142:131.
 53. SILBERBERG, R., M. SILBERBERG, A. VOGEL, and W. WETTSTEIN. 1961. Ultrastructure of articular cartilage of mice of various ages. *Am. J. Anat.* 109:251.
 54. FERNANDO, N. V. P., and H. Z. MOVAT. 1963. Fibrillogenesis in regenerating tendon. *Lab. Invest.* 12:214.
 55. PEACH, R., G. WILLIAMS, and J. A. CHAPMAN. 1961. A light and electron optical study of regenerating tendon. *Am. J. Pathol.* 38:495.
 56. ROSS, M. H. 1962. Some aspects of collagen fibrogenesis observed in the adrenal glands of young rats. In *Electron Microscopy: Fifth International Congress on Electron Microscopy Held in Philadelphia, Pennsylvania, August 29th to September 5th 1962*. S. S. Breese, Jr., editor. New York. 2:T-13.
 57. ROSS, R., and E. P. BENDITT. 1961. Wound healing and collagen formation. 1. Sequential changes in components of guinea pig skin wounds observed in the electron microscope. *J. Biophys. Biochem. Cytol.* 11:677.
 58. MATUKAS, V. J., B. J. PANNER, and J. L. ORBISON. 1967. Studies on ultrastructural identification and distribution of protein-polysaccharide in cartilage matrix. *J. Cell Biol.* 32:365.
 59. FERNÁNDEZ-MORÁN, H., and A. ENGSTRÖM. 1956. Ultrastructural organization of bone. *Nature.* 178:494.
 60. GLIMCHER, M. J., E. J. DANIEL, D. J. TRAVIS, and S. KAMHI. 1965. Electron optical and X-Ray diffraction studies of the organization of the inorganic crystals in embryonic bovine enamel. *J. Ultrastruct. Res. Suppl.* 7. 1.
 61. JOHANSEN, E., and H. F. PARKS. 1960. Electron microscopic observations on the three-dimensional morphology of apatite crystallites of human dentine and bone. *J. Biophys. Biochem. Cytol.* 7:743.
 62. ROBINSON, R. A. 1952. An electron-microscopic study of the crystalline inorganic component of bone and its relationship to the organic matrix. *J. Bone. Joint Surg.* 34A:389.